THE STABILITY OF PERIODIC ORBITS IN THE THREE-BODY PROBLEM

JOHN D. HADJIDEMETRIOU
University of Thessaloniki, Thessaloniki, Greece

(Received 11 June, 1974)

Abstract. A method is developed to study the stability of periodic motions of the three-body problem in a rotating frame of reference, based on the notion of surface of section. The method is linear and involves the computation of a 4×4 variational matrix by integrating numerically the differential equations for time intervals of the order of a period. Several properties of this matrix are proved and also it is shown that for a symmetric periodic motion it can be computed by integrating for half the period only.

This linear stability analysis is used to study the stability of a family of periodic motions of three bodies with equal masses, in a rotating frame of reference. This family represents motion such that two bodies revolve around each other and the third body revolves around this binary system in the same direction to a distance which varies along the members of the family. It was found that a large part of the family, corresponding to the case where the distance of the third body from the binary system is larger than the dimensions of the binary system, represents stable motion. The nonlinear effects to the linear stability analysis are studied by computing the intersections of several perturbed orbits with the surface of section $y_3=0$. In some cases more than 1000 intersections are computed. These numerical results indicate that linear stability implies stability to all orders, and this is true for quite large perturbations.

1. Introduction

It can be proved (Hadjidemetriou, 1975) that families of periodic orbits of the three-body problem, for fixed masses of the three bodies, can be obtained as a continuation of periodic orbits of the restricted circular three-body problem. These orbits are in a rotating frame of reference G_1xy whose origin coincides with the center of mass G_1 of the two bodies P_1, P_2, with masses m_1, m_2, respectively and its x-axis contains always these bodies. The existence of these periodic orbits has been proved for sufficiently small masses m_3 of the third body P_3. These periodic orbits have been continued numerically (Hadjidemetriou and Christides, 1975) by varying the mass m_3 and in this way periodic orbits of the three-body problem were obtained for the case where all three masses are of the same order of magnitude. Also, Hénon (1974a) has shown that families of periodic orbits for fixed masses of the three bodies exist. The aim of the present paper is to develop a method to study the stability of the periodic orbits of the three-body problem. The method is based on the notion of surface of section of Poincaré (e.g. Siegel and Moser, 1971; Szebehely, 1967) and is similar to the one developed by Hénon (1965) for the case of two degrees of freedom.

We assume that the center of mass of the three-body system is at rest with respect to an inertial frame and choose as generalized coordinates the coordinates x_1 of P_1 and x_3, y_3 of P_3, with respect to G_1xy and the angle ϑ between the x axis and a fixed

Celestial Mechanics **12** (1975) 255–276. *All Rights Reserved*

direction in the inertial frame. Then the Lagrangian of the system is

$$L = \tfrac{1}{2}(m_1 + m_2)\left\{q(\dot{x}_1^2 + x_1^2\dot{\vartheta}^2) + \frac{m_3}{m}[\dot{x}_3^2 + \dot{y}_3^2 + \dot{\vartheta}^2(x_3^2 + y_3^2) + \right.$$
$$\left. + 2\dot{\vartheta}(x_3\dot{y}_3 - \dot{x}_3y_3)]\right\} - V, \tag{1}$$

where

$$V = -\frac{Gm_1m_3}{r_{13}} - \frac{Gm_2m_3}{r_{23}} - \frac{Gm_1m_2}{r_{12}}, \tag{2}$$

$$m = m_1 + m_2 + m_3, \qquad q = m_1/m_2, \tag{3}$$

r_{ij} are the distances between the bodies P_i, P_j and G is the gravitational constant.

We note that the angle ϑ is ignorable, and consequently we have the angular momentum integral $\partial L/\partial\dot{\vartheta} = p = \text{constant}$, from which we obtain

$$\dot{\vartheta} = \frac{\dfrac{p}{m_1 + m_2} - \dfrac{m_3}{m}(x_3\dot{y}_3 - \dot{x}_3y_3)}{qx_1^2 + \dfrac{m_3}{m}(x_3^2 + y_3^2)}. \tag{4}$$

Also, due to the fact that $\partial L/\partial t = 0$, the energy integral exists. With the help of (4) the angle ϑ can be eliminated and the problem can be reduced to a problem with three degrees of freedom (Whittaker, 1960; Pars, 1965) with generalized coordinates the abscissa x_1 of P_1 and the coordinates x_3, y_3 of P_3 with respect to G_1xy. The corresponding Lagrangian is the Routhian function

$$R = \tfrac{1}{2}(m_1 + m_2)\left\{q\dot{x}_1^2 + \frac{m_3}{m}(\dot{x}_3^2 + \dot{y}_3^2) - \right.$$
$$\left. - \frac{\left[\dfrac{p}{m_1 + m_2} - \dfrac{m_3}{m}(x_3\dot{y}_3 - \dot{x}_3y_3)\right]^2}{qx_1^2 + \dfrac{m_3}{m}(x_3^2 + y_3^2)}\right\} - V. \tag{5}$$

The energy integral in this reduced three degree of freedom problem is of the form

$$E = f(x_1, x_3, y_3, \dot{x}_1, \dot{x}_3, \dot{y}_3, p) = \text{constant}. \tag{6}$$

This is a hypersurface in the six dimensional phase space x_1, x_3, y_3, $\dot{x}_1$, $\dot{x}_3$, $\dot{y}_3$. Consequently, any trajectory in phase space lies in this hypersurface.

2. Isoenergetic Displacements

Let us assume now that, for a fixed value of the angular momentum p in the Routhian (5), the initial conditions

$$\begin{aligned} x_1 &= x_{100}, & x_3 &= x_{300}, & y_3 &= 0, \\ \dot{x}_1 &= 0, & \dot{x}_3 &= 0, & \dot{y}_3 &= \dot{y}_{300} \end{aligned} \tag{7}$$

correspond to a symmetric periodic orbit. These initial conditions imply a certain value for the energy. Keeping always the same value for p, we consider a neighboring orbit with initial conditions

$$\begin{aligned} &x_{10} = x_{100} + \xi_{10}, \qquad x_{30} = x_{300} + \xi_{20}, \qquad y_{30} = 0, \\ &\dot{x}_{10} = \xi_{30}, \qquad \dot{x}_{30} = \xi_{40}, \end{aligned} \tag{8}$$

and $\dot{y}_3 = \dot{y}_{30}$ such that this orbit has the same energy constant as the periodic orbit (7). The trajectory in phase space of this latter orbit lies in the same hypersurface (6) as the periodic orbit (7). We take now the intersections of this orbit with the surface of section $y_3 = 0$. Let

$$x_1 = x_{100} + \xi_1, \qquad x_3 = x_{300} + \xi_2, \qquad \dot{x}_1 = \xi_3, \qquad \dot{x}_3 = \xi_4 \tag{9}$$

be the values of x_1, x_3, $\dot{x}_1$, $\dot{x}_3$ when y_3 becomes again equal to zero (and the orbit crosses the surface of section $y_3 = 0$ in the same direction as initially). Also, the value of $\dot{y}_3$ is readily obtained from the energy integral (6). In this way a transformation T is established in the four dimensional space x_1, x_3, $\dot{x}_1$, $\dot{x}_3$, between the point $Q_0(x_{10}, x_{30}, \dot{x}_{10}, \dot{x}_{30})$ and the point $Q_1(x_1, x_3, \dot{x}_1, \dot{x}_3)$, which is expressed in the form

$$\begin{aligned} x_1 &= g_1(x_{10}, x_{30}, \dot{x}_{10}, \dot{x}_{30}), \\ x_3 &= g_2(x_{10}, x_{30}, \dot{x}_{10}, \dot{x}_{30}), \\ \dot{x}_1 &= g_3(x_{10}, x_{30}, \dot{x}_{10}, \dot{x}_{30}), \\ \dot{x}_3 &= g_4(x_{10}, x_{30}, \dot{x}_{10}, \dot{x}_{30}), \end{aligned} \tag{10}$$

or symbolically,

$$Q_1 = TQ_0. \tag{11}$$

It is evident that the fixed points of this transformation correspond to periodic orbits. If now we repeat the above transformation n times we obtain a point Q_n given by

$$Q_n = T^n Q_0.$$

Thus, the stability of the considered periodic orbit with respect to isoenergetic displacements depends on the properties of the transformation T.

We shall linearize now the transformation T. For this reason we substitute (8) and (9) in (10) and obtain, to first order terms in ξ_{i0}, ξ_i,

$$\xi_i = \sum_{j=1}^{4} a_{ij}\xi_{j0}, \qquad (i = 1,\ldots, 4) \tag{12a}$$

or, in matrix form

$$\xi = A\xi_0, \tag{12b}$$

where ξ, ξ_0 are column vectors with elements ξ_i, ξ_{i0}, respectively and A is a 4×4 matrix with elements a_{ij}. The a_{ij} are the partial derivatives of the functions g_i with respect to x_1, x_3, $\dot{x}_1$, $\dot{x}_3$, evaluated for the initial conditions (7) of the periodic orbit. Equations (12) express the deviations of the neighboring orbit from the periodic orbit at the first crossing with the surface of section, in terms of the original deviations. Evidently, the deviations at the n-th crossing are given by $A^n\xi_0$. Thus the linear stability characteristics of the considered periodic orbit depend on the eigenvalues of the matrix A. The determinant of this matrix is in fact the Jacobian of the transformation T evaluated at the initial conditions (7) of the periodic orbit,

$$\det(A) = \frac{D(x_1, x_3, \dot{x}_1, \dot{x}_3)}{D(x_{10}, x_{30}, \dot{x}_{10}, \dot{x}_{30})}. \tag{13}$$

3. Properties of the Jacobian Matrix A

The variables x_1, x_3, $\dot{x}_1$, $\dot{x}_3$ are not canonical variables. It is evident however that the considered dynamical system can be expressed in Hamiltonian form and let q_1, q_2, p_1, p_2 be the corresponding canonical variables. Then the transformation T, given by (11), can be expressed in the canonical variables as

$$Q_1^c = T^c Q_0^c, \tag{14}$$

where T^c is the operator representing the mapping T in canonical variables and Q_0^c, Q_1^c the points Q_0, Q_1 expressed in canonical coordinates. The Jacobian determinant corresponding to this transformation is

$$\det(A^c) = \frac{D(q_1, q_2, p_1, p_2)}{D(q_{10}, q_{20}, p_{10}, p_{20})}. \tag{15}$$

By a known property of functional determinants we have

$$\frac{D(x_1, x_3, \dot{x}_1, \dot{x}_3)}{D(x_{10}, x_{30}, \dot{x}_{10}, \dot{x}_{30})} = \frac{D(x_1, x_3, \dot{x}_1, \dot{x}_3)}{D(q_1, q_2, p_1, p_2)} \times \\ \times \frac{D(q_1, q_2, p_1, p_2)}{D(q_{10}, q_{20}, p_{10}, p_{20})} \times \frac{D(q_{10}, q_{20}, p_{10}, p_{20})}{D(x_{10}, x_{30}, \dot{x}_{10}, \dot{x}_{30})} \tag{16}$$

or, using (13) and (15),

$$\det(A) = \det(A^c) \frac{\dfrac{D(x_1, x_3, \dot{x}_1, \dot{x}_3)}{D(q_1, q_2, p_1, p_2)}}{\dfrac{D(x_{10}, x_{30}, \dot{x}_{10}, \dot{x}_{30})}{D(q_{10}, q_{20}, p_{10}, p_{20})}}. \tag{17}$$

Since the mapping T^c is volume preserving (Siegel and Moser, 1971) we have $\det(A^c) = 1$. Also, the functional determinants appearing in the numerator and the denominator at the right hand side of (17) correspond to the transformation between the variables x_1, x_3, $\dot{x}_1$, $\dot{x}_3$ and the canonical variables q_1, q_2, p_1, p_2 at the initial and final points respectively. Since however these two points are identical for the periodic orbit, we obtain finally from (17),

$$\det(A) = 1. \tag{18}$$

This relation implies that the transformation T, given by (10), is volume preserving. Equation (18) will be also proved later by a different method, without reference to canonical variables.

We shall use now the symmetry properties of the periodic orbit (7) to find several properties of the matrix A. It can be proved (Hadjidemetriou and Christides, 1975) that the transformation

$$x_1 \to x_1, \qquad x_3 \to x_3, \qquad \dot{x}_1 \to -\dot{x}_1, \qquad \dot{x}_3 \to -\dot{x}_3, \qquad t \to -t \tag{19}$$

leaves the system unchanged. This implies that if to the initial point $x_{10}, x_{30}, \dot{x}_{10}, \dot{x}_{30}$ of the neighboring orbit corresponds, by the mapping (11), the point $x_1, x_3, \dot{x}_1, \dot{x}_3$, and the point $x_1, x_3, -\dot{x}_1, -\dot{x}_3$ is taken as the initial point, the corresponding final point under the mapping (11) will be $x_{10}, x_{30}, -\dot{x}_{10}, -\dot{x}_{30}$. Thus, together with (10) the following relations hold:

$$\begin{aligned} x_{10} &= g_1(x_1, x_3, -\dot{x}_1, -\dot{x}_3), \\ x_{30} &= g_2(x_1, x_3, -\dot{x}_1, -\dot{x}_3), \\ \dot{x}_{10} &= -g_3(x_1, x_3, -\dot{x}_1, -\dot{x}_3), \\ \dot{x}_{30} &= -g_4(x_1, x_3, -\dot{x}_1, -x_3), \end{aligned} \tag{20}$$

The linearized form of (20) is obtained in the same way as (12) and in matrix form is

$$\xi_0 = (JAJ)\xi, \tag{21}$$

where

$$J = \begin{pmatrix} 1 & 0 & 0 & 0 \\ 0 & 1 & 0 & 0 \\ 0 & 0 & -1 & 0 \\ 0 & 0 & 0 & -1 \end{pmatrix} \tag{22}$$

and A is the same matrix as in (12b). Comparing now (12b) with (21) we readily obtain for the inverse of the matrix A,

$$A^{-1} = JAJ. \tag{23}$$

We write now the matrix A in the form

$$A = \begin{pmatrix} A_1 & A_2 \\ A_3 & A_4 \end{pmatrix}, \tag{24}$$

where the A_i's are 2×2 matrices. Then, from (23) we obtain

$$A^{-1} = \begin{pmatrix} A_1 & -A_2 \\ -A_3 & A_4 \end{pmatrix} \tag{25}$$

from which the relations

$$\begin{aligned} A_1^2 - A_2A_3 &= I, \qquad & A_1A_2 &= A_2A_4, \\ A_3A_1 &= A_4A_3, \qquad & -A_3A_2 + A_4^2 &= I \end{aligned} \tag{26}$$

are readily obtained. The second relation of (26) is expressed in the form

$$A_1 = A_2 A_4 A_2^{-1}, \tag{27}$$

provided $\det(A_2) \neq 0$. This latter relation is a similarity transformation which implies

$$\det(A_1) = \det(A_4),$$
$$\operatorname{trace}(A_1) = \operatorname{trace}(A_4),$$

or, explicitly,

$$\begin{vmatrix} a_{11} & a_{12} \\ a_{21} & a_{22} \end{vmatrix} = \begin{vmatrix} a_{33} & a_{34} \\ a_{43} & a_{44} \end{vmatrix}, \tag{28}$$

$$a_{11} + a_{22} = a_{33} + a_{44}. \tag{29}$$

Equations (28) and (29) can be also obtained from the third relation (26).

Next, we multiply relation (23) from the left and the right with the matrix K, where

$$K = \begin{pmatrix} 1 & 0 & 0 & 0 \\ 0 & 0 & 1 & 0 \\ 0 & 1 & 0 & 0 \\ 0 & 0 & 0 & 1 \end{pmatrix}, \tag{30}$$

thus obtaining

$$KA^{-1}K = KJAJK,$$

and because $K^{-1} = K$,

$$(KAK)^{-1} = KJAJK.$$

This latter relation, written in block form is expressed as

$$\begin{pmatrix} B_1 & B_2 \\ B_3 & B_4 \end{pmatrix}^{-1} = \begin{pmatrix} J_1 B_1 J_1 & J_1 B_2 J_1 \\ J_1 B_3 J_1 & J_1 B_4 J_1 \end{pmatrix}, \tag{31}$$

where

$$\begin{gathered} B_1 = \begin{pmatrix} a_{11} & a_{13} \\ a_{31} & a_{33} \end{pmatrix}, \quad B_2 = \begin{pmatrix} a_{12} & a_{14} \\ a_{32} & a_{34} \end{pmatrix}, \quad B_3 = \begin{pmatrix} a_{21} & a_{23} \\ a_{41} & a_{43} \end{pmatrix}, \\ B_4 = \begin{pmatrix} a_{22} & a_{24} \\ a_{42} & a_{44} \end{pmatrix}, \quad J_1 = \begin{pmatrix} 1 & 0 \\ 0 & -1 \end{pmatrix}. \end{gathered} \tag{32}$$

From (31) we obtain, among others, the relation

$$B_1 J_1 B_2 J_1 + B_2 J_1 B_4 J_1 = 0,$$

or

$$(-B_1 J_1) = B_2 (J_1 B_4) B_2^{-1}.$$

From this relation we obtain

$$\det(B_1) = \det(B_4),$$

or explicitly,

$$\begin{vmatrix} a_{11} & a_{13} \\ a_{31} & a_{33} \end{vmatrix} = \begin{vmatrix} a_{22} & a_{24} \\ a_{42} & a_{44} \end{vmatrix}. \tag{33}$$

The equality of traces of $(-B_1J_1)$ and (J_1B_4) gives the relation (29).

Finally, if we multiply the relation (23) from the left and the right with the matrix M,

$$M = \begin{pmatrix} 1 & 0 & 0 & 0 \\ 0 & 0 & 0 & 1 \\ 0 & 0 & 1 & 0 \\ 0 & 1 & 0 & 0 \end{pmatrix}, \tag{34}$$

we obtain the relation, using the fact that $M^{-1}=M$,

$$(MAM)^{-1} = MJAJM. \tag{35}$$

If now we work as above, we obtain the relation

$$\begin{vmatrix} a_{11} & a_{14} \\ a_{41} & a_{44} \end{vmatrix} = \begin{vmatrix} a_{22} & a_{23} \\ a_{32} & a_{33} \end{vmatrix}. \tag{36}$$

We note also that the diagonal elements of JAJ in (23) are a_{11}, a_{22}, a_{33}, a_{44}. If now we take into account that $\det(A)=1$ and use the general formula $(-1)^{i+j}A_{ji}/|A|$ for the elements of the inverse of the matrix A, where A_{ij} are the minors of A, we obtain from (23) the relations

$$a_{ii} = A_{ii} \qquad (i = 1,\ldots, 4) \tag{37}$$

and consequently

$$\mathrm{trace}(A) = A_{11} + A_{22} + A_{33} + A_{44}. \tag{38}$$

4. Linear Stability of Periodic Orbits

As mentioned above, the linear isoenergetic stability of a periodic orbit of the three-body problem depends on the eigenvalues of the Jacobian matrix A. This is a 4×4 matrix and its characteristic equation is

$$\lambda^4 + \alpha\lambda^3 + \beta\lambda^2 + \gamma\lambda + \delta = 0, \tag{39}$$

where

$$\alpha = -\mathrm{trace}(A), \tag{40}$$

$$\beta = \begin{vmatrix} a_{11} & a_{12} \\ a_{21} & a_{22} \end{vmatrix} + \begin{vmatrix} a_{11} & a_{13} \\ a_{31} & a_{33} \end{vmatrix} + \begin{vmatrix} a_{11} & a_{14} \\ a_{41} & a_{44} \end{vmatrix} + \\ + \begin{vmatrix} a_{22} & a_{23} \\ a_{32} & a_{33} \end{vmatrix} + \begin{vmatrix} a_{22} & a_{24} \\ a_{42} & a_{44} \end{vmatrix} + \begin{vmatrix} a_{33} & a_{34} \\ a_{43} & a_{44} \end{vmatrix}, \tag{41}$$

$$\gamma = -(A_{11} + A_{22} + A_{33} + A_{44}), \tag{42}$$

$$\delta = \det(A). \tag{43}$$

If now we make use of the properties (18) and (38), we find that $\alpha=\gamma$, $\delta=1$, and consequently the characteristic equation (39) is a reciprocal equation of the form

$$\lambda^4 + \alpha\lambda^3 + \beta\lambda^2 + \alpha\lambda + 1 = 0. \tag{44}$$

If λ_1, λ_2, λ_3, λ_4 are the roots of this equation, they obey the relations

$$\lambda_1\lambda_2 = 1, \qquad \lambda_3\lambda_4 = 1. \tag{45}$$

That the eigenvalues of the matrix A can be arranged in reciprocal pairs can be also obtained directly from the relation (23). Consequently, the equation (44) can be expressed in the form

$$(\lambda^2 + b_1\lambda + 1)(\lambda^2 + b_2\lambda + 1) = 0, \tag{46}$$

where

$$b_1 = \tfrac{1}{2}(\alpha + \sqrt{\Delta}), \qquad b_2 = \tfrac{1}{2}(\alpha - \sqrt{\Delta}) \tag{47}$$

and

$$\Delta = \alpha^2 - 4(\beta - 2). \tag{48}$$

In order for the periodic orbit to be stable, all the eigenvalues λ_i of the transformation (12) must have a modulus not greater than unity. It is obvious however that this is not the case when two or all the λ_i are real, as can be seen from (45). A characteristic equation of the form (44) appears also in the case of the elliptic restricted three-body problem, where a complete study of the stability characteristics was made by Broucke (1969). It is found that there exist seven stability regions, only one of which corresponds to stable motion. Applying Broucke's analysis we find that the motion is stable when all the roots of (44) are complex conjugate lying on the unit circle, and this happens when the following three inequalities hold:

$$\Delta > 0, \qquad |b_1| < 2, \qquad |b_2| < 2. \tag{49}$$

In all other cases the motion is unstable.

A similar situation appears in the study of the stability of periodic orbits of the three dimensional restricted three-body problem where the problem reduces to the study of a characteristic equation of the form (44), studied by Bray and Goudas (1967). However, the condition $\Delta < 0$ for stability, contained in that paper is not correct as, in general, $\Delta < 0$ corresponds to unstable motion.

5. Numerical Computation of the Matrix A

The elements of the matrix A are the derivatives of the functions g_i in (10) with respect to the initial conditions, given by

$$\begin{aligned} &a_{i1} = \partial g_i/\partial x_{10}, \qquad a_{i2} = \partial g_i/\partial x_{30}, \qquad a_{i3} = \partial g_i/\partial \dot{x}_{10}, \\ &a_{i4} = \partial g_i/\partial \dot{x}_{30} \qquad (i = 1, \ldots, 4). \end{aligned} \tag{50}$$

Thus, the elements a_{ij} can be computed by giving successively small increments in the initial conditions of the periodic orbit (7) and performing the integration of the system of differential equations, until y_3 becomes again equal to zero and the sign of $\dot{y}_3$ is the same as $\dot{y}_{30}$. The value of the angular momentum constant p is fixed, equal to its value corresponding to the periodic orbit and the value of $\dot{y}_{30}$ is such that the energy is equal to that of the periodic orbit. Obviously, $y_{30}=0$ in all cases. The ratio of the initial and the final displacements of a variable from the initial conditions (7) of the periodic orbit gives the corresponding partial derivative.

The computation of the matrix A requires four integrations, each corresponding to a small increment in one of the initial values x_{10}, x_{30}, $\dot{x}_{10}$, $\dot{x}_{30}$ corresponding to the periodic orbit. In computing the elements of A, the relations (18), (28), (29), (33), (36) and (37) can be used to check the accuracy of the computations. In most cases studied, an increment of the order of 10^{-5} in the initial conditions x_{10}, x_{30}, $\dot{x}_{10}$, $\dot{x}_{30}$ gave satisfactory results (the accuracy of the integration was of the order of 10^{-11}). As a rule, the elements of A were obtained with an accuracy of at least four significant figures. A smaller or a larger increment resulted in poorer accuracy in the computation of the matrix A. It is evident that in order for the accuracy of A to be increased, the accuracy of the numerical computations must be increased.

The properties (18), (28), (29), (33), (36) and (37) of the matrix A allow us to reduce to three the number of additional integrations in order to obtain A. This is so because from these properties we readily find that the coefficients α and β in (43) can be obtained in terms of the elements a_{ij} for $i, j=1, 2, 3$ only. Indeed, from (29) and (40) we obtain

$$\alpha = -\operatorname{trace}(A) = -2(a_{11} + a_{22}) \tag{51}$$

and also β, because of (28), (33), (36) and (41) is given by

$$\beta = 2\left\{ \begin{vmatrix} a_{11} & a_{12} \\ a_{21} & a_{22} \end{vmatrix} + \begin{vmatrix} a_{11} & a_{13} \\ a_{31} & a_{33} \end{vmatrix} + \begin{vmatrix} a_{22} & a_{23} \\ a_{32} & a_{33} \end{vmatrix} \right\}. \tag{52}$$

Still we have a means to check the accuracy of the computations because from (29) and (37) we obtain the relation

$$A_{44} = a_{11} + a_{22} - a_{33} \tag{53}$$

which involves the elements a_{ij} with $i, j=1, 2, 3$ only and consequently it can serve as a check of the accuracy of A.

6. Computation of A by Integrating for Half the Period Only

In the previous paragraph the integrations required for the computation of the elements of the matrix A were carried out for a time interval about equal to the period of the periodic motion of the three-body problem. We shall prove now that the matrix A corresponding to a symmetric periodic orbit, can be obtained by performing the above mentioned four additional integrations for half the period only.

Let Q_0 with coordinates x_{10}, x_{30}, $\dot{x}_{10}$, $\dot{x}_{30}$ be the initial point of intersection with the surface of section $y_3=0$ of a neighboring orbit to the periodic orbit (7), corresponding to an isoenergetic displacement. After about one period there is another point of intersection Q, with coordinates x_1, x_3, $\dot{x}_1$, $\dot{x}_3$, where the intersection is in the same direction as initially. Between these two points of intersection there is another point of intersection Q', with coordinates x_1', x_3', $\dot{x}_1'$, $\dot{x}_3'$, where in this latter case the intersection is in the opposite direction than initially. For the two consecutive points of intersection with opposite direction there is a transformation similar to the transformation (10) which can be written in the form

$$
\begin{aligned}
x_1' &= h_1(x_{10}, x_{30}, \dot{x}_{10}, \dot{x}_{30}),\\
x_3' &= h_2(x_{10}, x_{30}, \dot{x}_{10}, \dot{x}_{30}),\\
\dot{x}_1' &= h_3(x_{10}, x_{30}, \dot{x}_{10}, \dot{x}_{30}),\\
\dot{x}_3' &= h_4(x_{10}, x_{30}, \dot{x}_{10}, \dot{x}_{30}),
\end{aligned}
\tag{54}
$$

for the transformation between the points Q_0 and Q'. If the point Q' is taken as the initial point, the final point is Q and their coordinates are related by

$$
\begin{aligned}
x_1 &= h_1'(x_1', x_3', \dot{x}_1', \dot{x}_3'),\\
x_3 &= h_2'(x_1', x_3', \dot{x}_1', \dot{x}_3'),\\
\dot{x}_1 &= h_3'(x_1', x_3', \dot{x}_1', \dot{x}_3'),\\
\dot{x}_3 &= h_4'(x_1', x_3', \dot{x}_1', \dot{x}_3').
\end{aligned}
\tag{55}
$$

We consider now small isoenergetic displacements from the periodic orbit (7) and express the coordinates of Q_0 and Q in the form (8) and (9), respectively and also the coordinates of Q' in the form

$$
x_1' = x_{100}' + \xi_1', \qquad x_3' = x_{300}' + \xi_2', \qquad \dot{x}_1 = \xi_3', \qquad \dot{x}_3' = \xi_4', \tag{56}
$$

where

$$
x_1 = x_{100}', \qquad x_3 = x_{300}', \qquad \dot{x}_1 = 0, \qquad \dot{x}_3 = 0, \tag{57}
$$

are the coordinates of the point of intersection of the periodic orbit with the $y_3=0$ plane at half the period. Using (8), (9) and (56), the transformations (54) and (55) take the linearized form

$$
\xi' = B_1\xi_0, \qquad \xi = B_2\xi', \tag{58}
$$

where ξ_0, ξ', ξ are column vectors with elements ξ_{i0}, ξ'_i, ξ_i respectively and B_1, B_2 are 4×4 matrices with elements the partial derivatives of the functions h_i, h'_i with respect to the variables x_1, x_3, $\dot{x}_1$, $\dot{x}_3$, respectively. The matrix B_1 is computed for the initial conditions $x_1=x_{100}$, $x_3=x_{300}$, $\dot{x}_1=0$, $\dot{x}_3=0$ at $t=0$ and the matrix B_2 is computed for the values $x_1=x'_{100}$, $x_3=x'_{300}$, $\dot{x}_1=0$, $\dot{x}_3=0$ of the periodic orbit at $t=\tau/2$, where τ is the period. From (58) we obtain

$$\xi = (B_2B_1)\xi_0 \tag{59}$$

and comparing with (12b) we readily obtain

$$A = B_2B_1. \tag{60}$$

We note now, due to the fact that the transformation (19) leaves the system of differential equations invariant, that if we take as initial point the point x_1, x_3, $-\dot{x}_1$, $-\dot{x}_3$, the point corresponding to the subsequent intersection (in the opposite direction) is x'_1, x'_3, $-\dot{x}'_1$, $-\dot{x}'_3$, and consequently they are related by a relation similar to (54),

$$\begin{aligned} x'_1 &= h_1(x_1, x_3, -\dot{x}_1, -\dot{x}_3),\\ x'_3 &= h_2(x_1, x_3, -\dot{x}_1, -\dot{x}_3),\\ \dot{x}'_1 &= -h_3(x_1, x_3, -\dot{x}_1, -\dot{x}_3),\\ \dot{x}'_3 &= -h_4(x_1, x_3, -\dot{x}_1, -\dot{x}_3). \end{aligned} \tag{61}$$

Also, if x'_1, x'_3, $-\dot{x}'_1$, $-\dot{x}'_3$ is taken as the initial point, the next point of the above mapping will be x_{10}, x_{30}, $-\dot{x}_{10}$, $-\dot{x}_{30}$, and these coordinates are related by

$$\begin{aligned} x_{10} &= h'_1(x'_1, x'_3, -\dot{x}'_1, -\dot{x}'_3),\\ x_{30} &= h'_2(x'_1, x'_3, -\dot{x}'_1, -\dot{x}'_3),\\ \dot{x}_{10} &= -h'_3(x'_1, x'_3, -\dot{x}'_1, -\dot{x}'_3),\\ \dot{x}_{30} &= -h'_4(x'_1, x'_3, -\dot{x}'_1, -\dot{x}'_3). \end{aligned} \tag{62}$$

Using (8), (9) and (56), we obtain the linearized form of the transformations (61) and (62),

$$\xi' = JB_1J\xi, \qquad \xi_0 = JB_2J\xi', \tag{63}$$

where the matrix J is given by (22). From (63) we obtain

$$\xi_0 = (JB_2B_1J)\xi, \tag{64}$$

because $J^2=I$. We compare now the second of (58) with the first of (63) and obtain $B_2^{-1}=JB_1J$, or using the fact that $J^{-1}=J$,

$$B_2 = JB_1^{-1}J. \tag{65}$$

We substitute now (65) in (60) and obtain finally

$$A = JB_1^{-1}JB_1. \tag{66}$$

This latter relation expresses the matrix A in terms of the matrix B_1, which involves integration for half the period only.

If we take into account that $\det(J)=1$, we obtain from (66) that $\det(A)=1$, a result already obtained earlier in a different method. We also note, using (60) and (64) that we find again the relation (23).

We shall prove now that

$$\det(B_1) = 1. \tag{67}$$

To do so we take into account that $\det(B_1)$ is the Jacobian determinant of the transformation (54),

$$\det(B_1) = \frac{D(x'_1, x'_3, \dot{x}'_1, \dot{x}'_3)}{D(x_{10}, x_{30}, \dot{x}_{10}, \dot{x}_{30})} \tag{68}$$

and working as in Section 3 we obtain finally

$$\det(B_1) = \det(B_1^c)\,\frac{\dfrac{D(x'_1, x'_3, \dot{x}'_1, \dot{x}'_3)}{D(q'_1, q'_2, p'_1, p'_2)}}{\dfrac{D(x_{10}, x_{30}, \dot{x}_{10}, \dot{x}_{30})}{D(q_{10}, q_{20}, p_{10}, p_{20})}}, \tag{69}$$

where $\det(B_1^c)$ is the corresponding Jacobian determinant in the canonical variables. By a corollary to Liouville's theorem (Pars, 1965) this transformation is volume preserving and consequently

$$\det(B_1^c) = 1. \tag{70}$$

If now we set

$$q_1 = x_1, \qquad q_2 = x_3, \tag{71}$$

the corresponding momenta are obtained from the Lagrangian R of the reduced system given by (5), for $y_3=0$, by

$$\begin{aligned} p_1 &= \left(\frac{\partial R}{\partial \dot{x}_1}\right)_{y_3=0} = q(m_1 + m_2)\dot{x}_1, \\ p_2 &= \left(\frac{\partial R}{\partial \dot{x}_3}\right)_{y_3=0} = \frac{m_3}{m}(m_1 + m_2)\dot{x}_3, \end{aligned} \tag{72}$$

where q and m are given by (3). From (71) and (72) it easily follows that the numerator and denominator at the right hand side of (69) are equal and consequently, using (70), we obtain finally the relation (67). The matrix B_1 involved in (66) can be computed numerically in the same way as the matrix A. A considerable amount of computing time is saved in computing the matrix A from (66). The accuracy in the numerical computation of B_1 can be checked by the relation (67). It should be emphasized however that the properties (18), (28), (29), (33) and (37) can no longer be used to check the accuracy in the computation of the matrix A. This is so because any matrix which is expressed in the form (66) has a determinant equal to unity and obeys the property

(23), which are the only properties used to find all the above mentioned relations for A. Thus, all the above properties of A will be verified identically no matter how large an error exists in the computation of B_1.

7. Numerical Results

The method to study the stability of periodic orbits of the three-body problem, developed above, will be applied now to study the stability of a family of periodic orbits corresponding to the case where all three masses are equal, $m_1=m_2=m_3$. One member of this family has been obtained by continuing numerically a periodic orbit of the restricted circular three-body problem by varying the mass m_3. This procedure is explained in detail in Hadjidemetriou and Christides (1975), and will not be repeated here. We have found it more convenient in practice to integrate the system of differential equations derived from the Lagrangian (1), where the angle ϑ is also included as one of the variables and not from the reduced Lagrangian (5). The normalization of the variables used is $m_1=m_2=m_3=\frac{1}{3}$, $G=1$, $\dot{\vartheta}_0=1$, where $\dot{\vartheta}_0$ is the initial angular velocity of the rotating frame. According to this normalization, the angular momentum p varies along the members of the family. Thus, in performing the additional integrations required to compute the elements of the matrix A, by giving small increments to the values of x_1, x_3, $\dot{x}_1$, $\dot{x}_3$ corresponding to the periodic orbit, we have to change $\dot{\vartheta}_0$ and $\dot{y}_{30}$ in such a way that the perturbed orbit has the same value of E and p.

In Table I we present the initial conditions of some of the periodic orbits of the above mentioned family. We also give in the same table the period, the energy, the angular momentum and the values of b_1, b_2 given by (46) and (47). Where no values are given for b_1 and b_2, it implies that $\Delta<0$. These initial conditions lie on a smooth space curve in the space $x_{10}x_{30}\dot{y}_{30}$ and its projections on the planes $x_{10}x_{30}$ and $x_{30}\dot{y}_{30}$ are presented in Figure 1 in two characteristic curves. On these characteristic curves the stability (S) or instability (U) is indicated. Also, in Figure 2 we present some of the orbits of the family in the rotating frame of reference G_1xy. The motion of the body P_1 in the x-axis is also indicated. The motion of the body P_2, which in this case is symmetric to that of P_1 with respect to the origin G_1, is not shown. As we proceed to the one end of the characteristic curves (part A) the three-body system tends to a binary system formed by the bodies P_1 and P_3 and the body P_2 moves around this binary in the same direction to a larger distance from it. The period decreases continuously towards this end and also the energy decreases. As we proceed to the other end of the characteristic curves (part C) the period and the energy increase. All orbits represented by the part AB are stable and from there on become unstable. The instability (measured by the magnitude of the eigenvalues of the matrix A) increases rapidly and the part around the point C represents highly unstable orbits. This fact, together with the large period of these orbits makes it difficult to continue the family as it is time consuming.

TABLE I

A family of periodic orbits with equal masses for all three bodies

x_{10}	x_{30}	$\dot{y}_{30}$	$\tau/2$	E	p	b_1	b_2	Stability
1.095 548 86	1.022 425 45	−2.946 375 05	0.076 672	−0.811 309 95	0.363 019 30	−1.9977	−1.9977	*S*
1.002 612 39	0.902 425 45	−2.479 571 63	0.123 789	−0.611 319 72	0.353 875 10	−1.9918	−1.9919	*S*
0.876 809 81	0.702 425 45	−1.782 102 71	0.292 671	−0.385 092 99	0.343 998 56	−1.9266	−1.9280	*S*
0.802 047 65	0.522 425 45	−1.271 638 02	0.640 001	−0.273 723 85	0.341 874 13	−1.5065	−1.5310	*S*
0.771 892 87	0.402 425 45	−0.998 106 93	1.092 636	−0.229 291 39	0.343 941 87	−0.3685	−0.6434	*S*
0.762 848 95	0.342 425 45	−0.889 881 42	1.504 882	−0.210 357 87	0.346 300 60	1.0163	0.0881	*S*
0.761 919 15	0.332 425 45	−0.876 149 09	1.610 221	−0.206 794 62	0.346 847 74	1.3755	0.2333	*S*
0.761 308 01	0.322 425 45	−0.865 506 86	1.743 966	−0.202 700 82	0.347 481 42	1.7757	0.4164	*S*
0.761 398 66	0.312 425 45	−0.862 504 90	1.950 458	−0.197 052 29	0.348 294 44	1.9276	0.9085	*S*
0.761 537 02	0.311 225 45	−0.863 604 33	1.989 432	−0.196 054 00	0.348 422 57	1.7211	1.1766	*S*
0.761 598 48	0.310 825 45	−0.864 148 96	2.004 173	−0.195 680 97	0.348 468 82	–	–	*U*
0.761 670 48	0.310 425 45	−0.864 816 37	2.020 124	−0.195 280 00	0.348 517 49	–	–	*U*
0.768 585 10	0.318 489 42	−0.947 188 71	2.669 244	−0.180 529 34	0.349 318 91	–	–	*U*
0.772 068 53	0.328 489 42	−0.988 688 62	2.875 031	−0.176 277 53	0.349 200 22	–	–	*U*
0.772 730 38	0.330 489 42	−0.996 390 09	2.911 089	−0.175 549 35	0.349 169 69	–	–	*U*
0.773 385 85	0.332 489 42	−1.003 954 35	2.946 047	−0.174 848 13	0.349 138 23	−5.0820	−10.5790	*U*
0.774 036 22	0.334 489 42	−1.011 396 99	2.980 052	−0.174 170 47	0.349 106 17	−4.5745	−12.7540	*U*
0.782 341 59	0.360 489 42	−1.100 901 60	3.371 221	−0.166 693 38	0.348 725 40	−3.3105	−37.0384	*U*
0.800 791 71	0.415 489 42	−1.268 813 23	4.092 251	−0.154 440 17	0.348 723 35	−2.9674	−83.1946	*U*
0.804 374 80	0.425 489 42	−1.297 684 83	4.219 792	−0.152 470 90	0.348 877 01	−2.9380	−89.8951	*U*
0.810 651 94	0.442 502 30	−1.346 057 58	4.437 199	−0.149 242 09	0.349 254 31	−2.9011	−99.8154	*U*
0.821 451 94	0.470 406 78	−1.423 837 73	4.797 651	−0.144 223 63	0.350 188 78	−2.8835	−111.5570	*U*
0.831 051 94	0.493 946 28	−1.488 394 80	5.107 752	−0.140 213 81	0.351 275 07	−2.9235	−117.0173	*U*
0.843 051 94	0.521 955 40	−1.564 442 75	5.486 094	−0.135 668 73	0.352 906 18	−3.0580	−118.3948	*U*
0.864 278 22	0.567 360 52	−1.689 734 93	6.139 448	−0.128 604 11	0.356 352 35	−3.5960	−110.4138	*U*
0.881 859 98	0.604 360 52	−1.787 208 60	6.671 667	−0.123 475 67	0.359 592 09	−4.4477	−97.1528	*U*

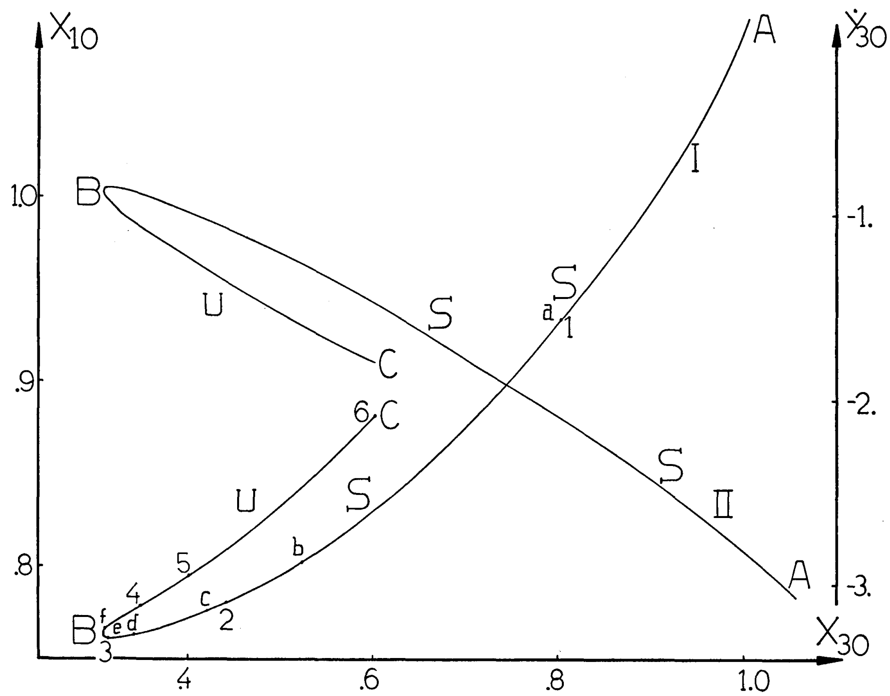

Fig. 1. Characteristic curves representing a family of symmetric periodic orbits with equal masses for all three bodies. Curve I corresponds to the relation $x_{30}-x_{10}$ and curve II to $x_{30}-\dot{y}_{30}$. The orbits represented in the part A–B are stable (S) and those in the part B–C are unstable (U).

8. The Effect of Nonlinear Terms

The stability discussed above is linear stability and consequently the analysis is valid for infinitesimal perturbations only. In order to study the case where the perturbation is finite (even large) we performed the numerical integration of the system of differential equations governing the three-body problem for several perturbed initial conditions along the above mentioned family. Both stable and unstable periodic orbits were used, whose initial conditions are represented by the letters a, b, c, d, e, f in the characteristic I of Figure 1. The orbits from a to e are linearly stable and the orbit f is unstable. We have studied in more detail perturbed orbits to the orbit a, which is far from the instability region and to the orbit e which is close to it. In these two cases more than 1000 points of intersection with the plane $y_3=0$ were computed. In all cases the perturbed orbits had the same energy and angular momentum as the corresponding periodic orbit. The accuracy of the computations was retained to ten decimal places throughout. We give below the results obtained from the numerical computations:

Orbit a. This periodic orbit corresponds to a close binary system formed by the bodies P_1 and P_3 and the third body P_2 revolves around this binary system, in the same direction, to a large distance compared to the dimensions of the close binary. This is a rather degenerate case as the effect of the body P_2 to the close binary P_1, P_3 is small. Several perturbed initial conditions have been used for the numerical

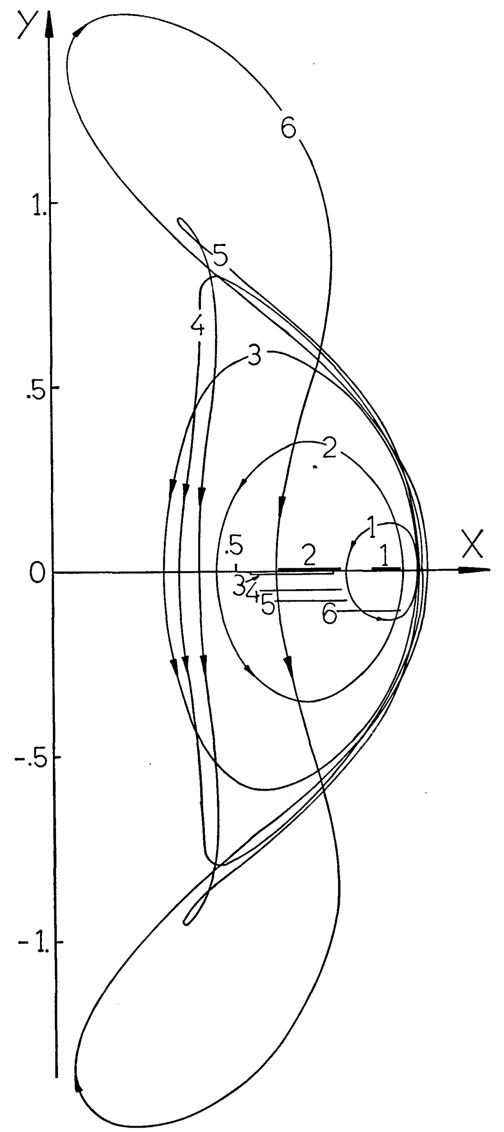

Fig. 2. Orbits belonging to the family of Figure 1, in the rotating frame G_1xy. The motion of P_2 on the x-axis (not shown) is symmetric to that of P_1, with respect to the origin. The motion of P_1 on the x-axis is indicated by straight lines parallel to the x-axis. The direction of motion of P_1 is opposite to that of the projection of P_3 on the x-axis. The initial conditions for each orbit are shown in Figure 1, (on the curve I only) at the corresponding number.

integrations, corresponding to deviations Δx_1, Δx_3, $\Delta \dot{x}_1$, $\Delta \dot{x}_3$ ranging from 0.01 to 0.10 (in the normalized units used in this paper). For a graphic illustration of the results obtained, we present in Figures 3 and 4 the projections of the points of intersection on the planes $x_1\dot{x}_1$ and $x_3\dot{x}_3$, for some typical cases. It turned out that in all cases these projections lie on smooth curves, which indicates that the points of intersection lie on a smooth curve in the four dimensional space $x_1x_3\dot{x}_1\dot{x}_3$.

In Figure 3a we have plotted the values $(x_1, \dot{x}_1)$ and in Figure 3b the values $(x_3, \dot{x}_3)$ of the tetrads mentioned above, for consecutive intersections of the perturbed orbit with the surface of section $y_3=0$, corresponding to a displacement from the stable periodic orbit

$$\begin{aligned} x_1 &= 0.940\,821\,152\,56, & x_3 &= 0.812\,425\,450\,00, \\ \dot{x}_1 &= 0, & \dot{x}_3 &= 0, \\ y_3 &= 0 & & \\ \dot{y}_3 &= -2.150\,687\,295\,28, & \dot{\vartheta} &= 1, \end{aligned} \tag{73}$$

given by

$$\Delta x_1 = \Delta x_3 = \Delta \dot{x}_1 = \Delta \dot{x}_3 = \varepsilon. \tag{74}$$

The values for the perturbation ε were $\varepsilon=0.02$, 0.04, 0.06, 0.10. The points $(x_1, \dot{x}_1)$, $(x_3, \dot{x}_3)$ at the consecutive intersections (in the same direction) with the surface of

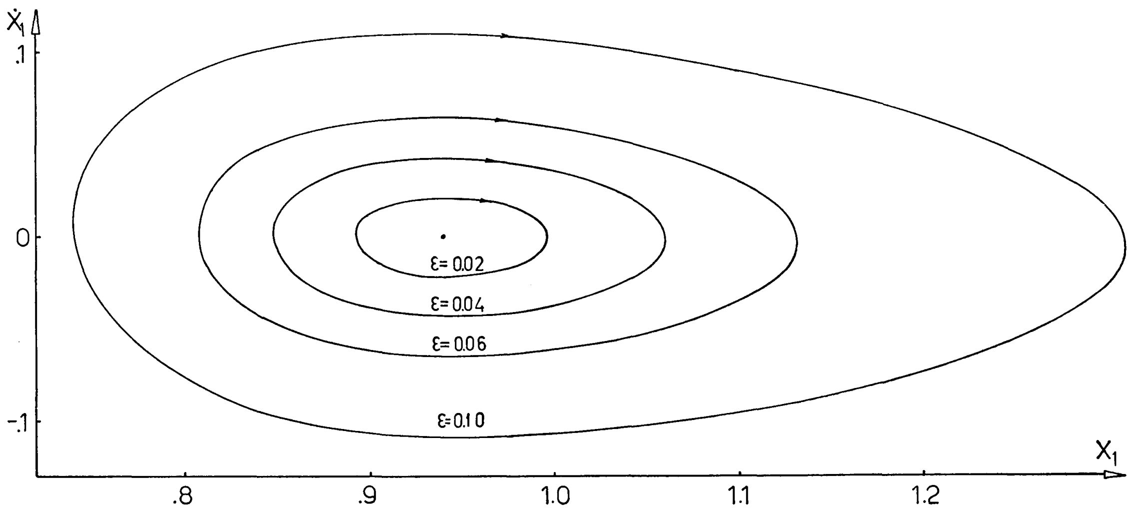

Fig. 3a.

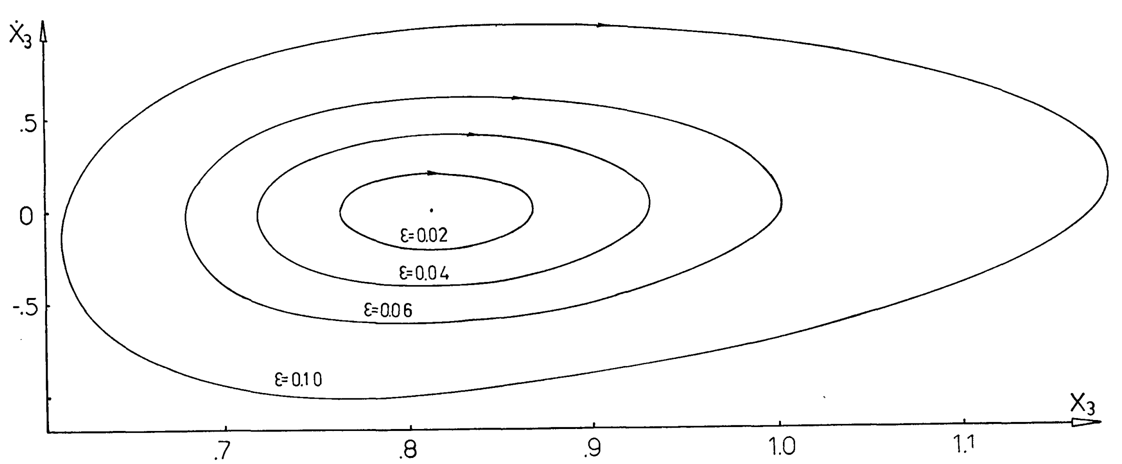

Fig. 3b.

Fig. 3a–b. Projections of consecutive points of intersection $(x_1, x_3, \dot{x}_1, \dot{x}_3)$ of the perturbed orbit (74) with the $y_3=0$ plane. (a) Projection to the $x_1\dot{x}_1$-plane. (b) Projection to the $x_3\dot{x}_3$-plane.

section $y_3 = 0$ are found to lie on smooth closed curves which we shall call *invariant curves*. The points on the invariant curves were ordered in such a way that consecutive points were placed one after the other. For small values of ε these curves are almost ellipses with the periodic orbit (73) lying at the center. For larger values of ε these ellipses are distorted. About 40 to 45 intersections (i.e. revolutions) were needed to obtain a complete invariant curve, depending on the value of ε. From that point on the tetrads corresponding to the subsequent intersections described again the same invariant curve.

The above picture however of invariant curves is not the general case. We have

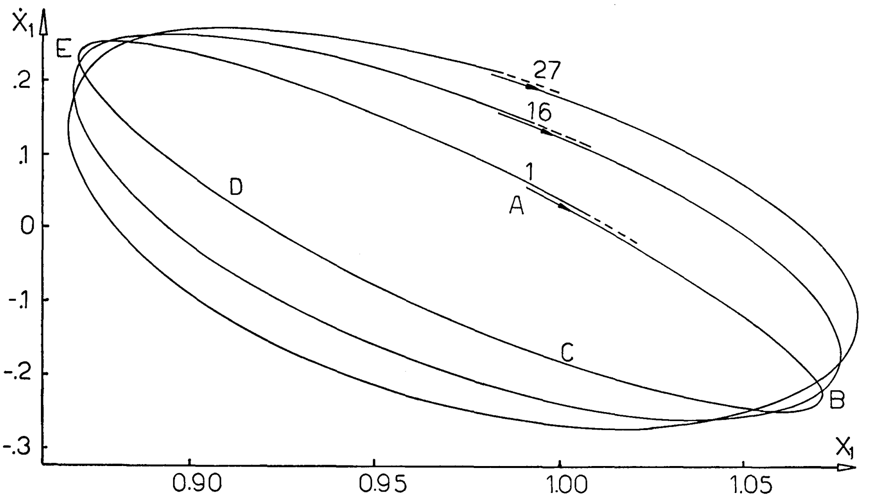

Fig. 4a.

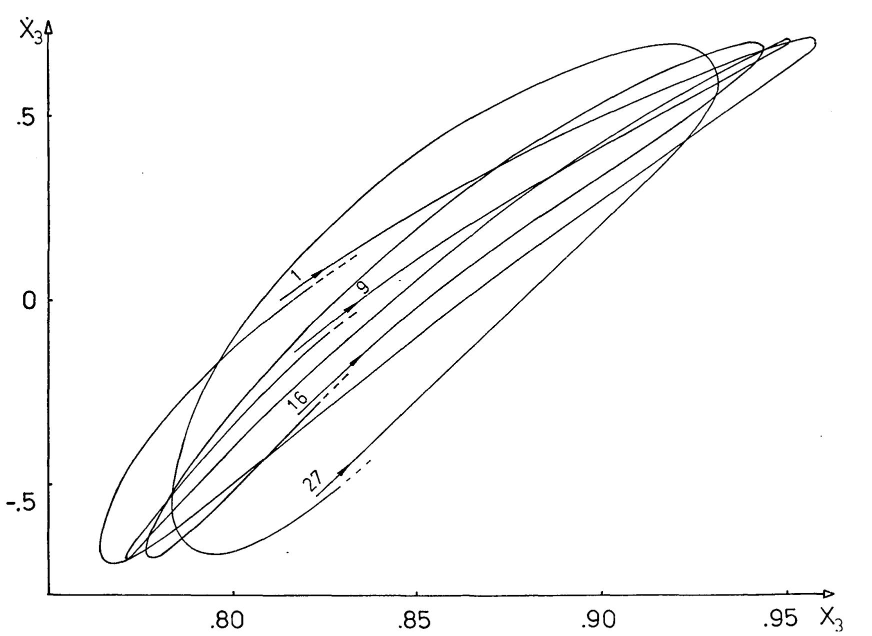

Fig. 4b.

Fig. 4a–b. Projections of the consecutive points of intersection $(x_1, x_3, \dot{x}_1, \dot{x}_3)$ of the perturbed orbit (75) with the $y_3 = 0$ plane. (a) Projection to the $x_1\dot{x}_1$-plane. (b) Projection to the $x_3\dot{x}_3$-plane.

performed the numerical integrations for several perturbed initial conditions close to those of the periodic orbit (73). In all cases the same qualitative results were obtained and we present them by a typical example corresponding to a perturbation

$$\Delta x_1 = \Delta \dot{x}_1 = 0.05, \qquad \Delta x_3 = \Delta \dot{x}_3 = 0. \tag{75}$$

The computations in this case were extended to about 1200 revolutions (periods) and the same number of intersections with the plane $y_3=0$ were obtained. The points of intersection $(x_1, x_3, \dot{x}_1, \dot{x}_3)$ are shown in Figures 4a, b. In Figure 4a we have plotted the consecutive points $(x_1, \dot{x}_1)$ and in Figure 4b the points $(x_3, \dot{x}_3)$. In both diagrams these points were found to lie on smooth curves which are ovals. However, contrary to the case (74), these ovals are not closed but almost closed. About 45 points were needed to obtain a complete oval and the consecutive points are ordered one after the other. In Figure 4a the ovals spiral out and in Figure 4b they spiral in initially and after about 500 periods, this phenomenon is reversed. To avoid complication of the figures, we have plotted in Figure 4a the first, the 16th and the 27th oval and in Figure 4b the 1st, 9th, 16th and 27th oval. The transition from spiralling in to spiralling out in Figure 4b is in the 9th and 10th oval. It is noted that the points $(x_3, \dot{x}_3)$ corresponding to the intersections of the perturbed orbit (75) with the plane $y_3=0$ fill all the space inside the initial oval. Also, a systematic slow rotation of the ovals was noted.

From the above results we have clear indications that linear stability implies in this case stability in general, and not only for very small perturbations.

Orbit b. This periodic orbit is denoted by the letter *b* in the characteristics of Figure 1. It is linearly stable and of the same type as orbit *a* but the body P_2 is now nearer to the binary system formed by P_1 and P_3. We performed the numerical integration for a perturbed orbit corresponding to $\Delta x_1=\Delta x_3=\Delta \dot{x}_1=\Delta \dot{x}_3=0.01$ and we plotted the projections of the points of intersection on the planes $x_1\dot{x}_1$ and $x_3\dot{x}_3$, as before. It was noted that these points do not lie any more on smooth curves but they appear as slightly diffused. The oval shape of the projected points is evident in this case too. Several hundred intersections were computed and from the results obtained it is indicated that the orbit is stable to all orders.

Orbit c. This periodic orbit is linearly stable and the only difference from orbit *b* is that the body P_2 is still closer to the binary system formed by P_1, P_3. The perturbation used was $\Delta x_1=\Delta x_3=\Delta \dot{x}_1=\Delta \dot{x}_3=0.01$ and the results are similar to those of orbit *b*. The diffusion of the 'invariant curves' is more evident but the oval shape of the whole configuration can still be easily seen. The results indicate complete stability.

Orbit d. The body P_2 is closer to the binary system formed by P_1P_3 than before and the orbit is linearly stable. The perturbation used was the same as in orbit *c*. The diffusion now is profound. The oval shape of the whole configuration can still be detected. The results indicate complete stability.

Orbit e. This orbit is linearly stable but on the verge of instability. For this reason it was studied in more detail. The distance of P_2 from the binary system P_1-P_3 is of the same order of magnitude as the dimensions of the binary system. We have computed two perturbed orbits corresponding to the perturbations $\Delta x_1=\Delta x_3=\Delta \dot{x}_1=\Delta \dot{x}_3=\varepsilon$ where $\varepsilon=0.01$, and $\varepsilon=0.10$, respectively. The results can be summarized as follows: (1) $\varepsilon=0.01$: About 1000 intersections (in the same direction) were computed. The diffusion is complete, the points lying in a bounded region in the space $x_1x_3\dot{x}_1\dot{x}_3$, and there is no indication of escape. The results suggest complete stability. The maximum deviations from the periodic orbit which were observed are: $\Delta x_1=\pm 0.05$, $\Delta x_3=\pm 0.03$, $\Delta \dot{x}_1=\pm 0.02$, $\Delta \dot{x}_3=\pm 0.05$. Deviations near the above maximum deviations appear randomly many times among the 1000 intersections computed. (2) $\varepsilon=0.10$: In this case the system disintegrates by forming a binary system between the bodies P_1, P_3 whose distance from the body P_2 tends to infinity. The continuous increase of the distance of P_2 from the binary system P_1-P_3 starts after about 300 points of intersection (in the same direction), during which period there is an interplay between the three bodies.

Orbit f. This is an unstable orbit. The perturbation given was $\Delta x_1=\Delta x_3=\Delta \dot{x}_1=\Delta \dot{x}_3=0.01$. The system disintegrates by forming a binary system between the bodies P_2-P_3 while the distance of P_1 from the binary P_2-P_3 tends to infinity. The continuous increase of the distance of P_1 from the binary P_2-P_3 starts after about 300 intersections (in the same direction).

9. Discussion

The stability of a periodic motion of the three-body problem studied above was for isoenergetic displacements only. It can be easily shown however that in general a periodic motion with energy E which is stable for isoenergetic displacements, is stable for the general case also. Let us consider a displacement from the initial conditions of a periodic motion which corresponds to a perturbed orbit with a different energy, E', than the original periodic orbit. If now we take into account that the given periodic motion belongs to a monoparametric family of periodic motions along which the energy varies, we can interpret the given displacement as an isoenergetic displacement from another periodic motion belonging to the same family which has an energy constant equal to E'. Taking into account that for small perturbations the periodic motion with energy E' is near the original periodic motion with energy E and the fact that the neighboring periodic motion with energy E' is isoenergetically stable, we come to the conclusion that isoenergetic stability of a periodic motion which belongs to a monoparametric family of periodic motions, along which the energy varies continuously, implies stability in general.

The stability analysis presented in Sections 2–4 is a linear analysis and consequently it is valid only for infinitesimal displacements. An attempt to study the nonlinear effects is made by the method of surfaces of section, which was applied to several members of the family of periodic motions given by Table I and Figure 1. The numerical results obtained indicate that linear stability implies complete stability. It was also noted that a perturbed orbit, during the course of its evolution, may deviate considerably from the original periodic orbit without the triple system to disintegrate. This type of motion was found by Szebehely and was called by him 'interplay'. In view of the above results we can say that this interplay can be considered as a perturbed motion to a stable periodic orbit. It must be also emphasized that the disintegration of the triple system may take place after several hundred intersections (periods) and for this reason great care should be taken in deciding whether or not a certain motion is stable or not.

The fact that the points of intersection around a stable periodic orbit, for sufficiently small perturbations, lie in a bounded region, suggest the existence of an additional integral of motion, valid near the periodic orbit.

Finally, we note that the family of periodic motions studied represents motion of three bodies with equal masses such that two of the bodies, P_1 and P_3, revolve around each other and the third body, P_2, revolves around this binary system to a distance which varies along the members of the family. The stability analysis has revealed that a considerable part of the family represents stable motion. The stability appears for that part of the family which corresponds to a motion of P_2 which is not very close to the binary system formed by P_1, P_3. The motion becomes unstable when the distance between P_2 and the binary system is of the order of the dimensions of the binary system. From these results we come to the conclusion that triple star systems with equal masses of all three stars can exist, provided that this triple system is composed of a binary system and a third star revolving around this binary system in the same direction to a distance which is larger than the dimensions of the binary system. Then the motion of the triple star system can be considered as a perturbed motion to a stable periodic motion of the kind studied in the present paper. On the contrary, one should not expect triple star systems with equal masses for all three stars, composed of a binary system and a third star revolving around this binary system in the same direction to a close distance, as such motions are proved to be unstable. These conclusions are in agreement with observations of triple star systems and they are qualitatively similar to results obtained by Harrington (1972) by numerical integrations.

Similar results concerning the stability of triple star systems were obtained by Hénon (1974b) who studied a family of periodic orbits with equal masses. Two of the bodies form a binary system and the third revolves around this binary system in the opposite direction than that of the revolution of the binary. The motion was found to be stable for a large part of the family, including cases where the three bodies are to a distance with each other of the same order of magnitude.

Acknowledgements

The author wishes to thank Dr Brouke and Dr Hénon for many useful comments as referees.

The numerical computations were made with the UNIVAC 1106 computer of the University of Thessaloniki.

References

Bray, T. A. and Goudas, C. L.: 1967, *Advances in Astronomy and Astrophysics*, Vol. 5, p. 111.
Brouke, R. A.: 1969, National Aeronautics and Space Administration, Technical Report 32–1360.
Hadjidemetriou, John D.: 1975, *Celes. Mech.*, in press.
Hadjidemetriou, John D. and Christides, Th.: 1975, *Celes. Mech.*, in press.
Harrington, R. S.: 1972, *Celes. Mech.* **6**, 322.
Hénon, M.: 1965, *Ann. Astrophys.* **28**, 992.
Hénon, M.: 1974a, *Celes. Mech.* **10**, 375.
Hénon, M.: 1974b, private communication.
Pars, L. S.: 1965, *A Treatise on Analytical Dynamics*, Heinemann, London, §10.1,22.
Siegel, C. L. and Moser, J.: 1971, *Lectures on Celestial Mechanics*, Springer-Verlag, Heidelberg, §22, 31.
Szebehely, V.: 1967, *Theory of Orbits*, Academic Press, New York, §9.10.
Whittaker, E. T.: 1960, *Analytical Dynamics of Particles and Rigid Bodies*, Cambridge Univ. Press, §38.